Elastic scattering of 210 MeV ^{6}Li ions from ^{12}C and ^{58}Ni and unique ^{6}Li-nucleus optical potentials

A. Nadasen, M. McMaster, G. Gunderson, A. Judd, and S. Villanueva
University of Michigan, Dearborn, Michigan 48128

P. Schwandt
Indiana University Cyclotron Facility, Bloomington, Indiana 47405

J. S. Winfield and J. van der Plicht*
National Superconducting Cyclotron Laboratory, Michigan State University, East Lansing, Michigan 48224

R. E. Warner
Oberlin College, Oberlin, Ohio 44074

F. D. Becchetti and J. W. Jänecke
University of Michigan, Ann Arbor, Michigan 48109
(Received 19 August 1987)

Angular distributions of the differential cross sections for the elastic scattering of 210 MeV ^{6}Li from ^{12}C (3°–61°) and ^{58}Ni (3°–48°) have been measured. The cross sections exhibit diffractive oscillations at small angles and exponential falloff characteristic of nuclear rainbow scattering at large angles. The data beyond the rainbow angle make it possible to obtain *unique* optical model potentials for the ^{6}Li + nucleus interaction, thus eliminating the discrete ambiguities inherent in the lower-energy studies. By truncating the angular distributions, data up to the rainbow angle could be fitted with several discrete ambiguous potentials. Extrapolation of the unique potentials to lower energies provides an energy dependence of the real potential volume integral given by $J_R/6A = J_R^0/6A - \beta \ln E_{\rm lab}$ with $J_R^0/6A \approx 800 \pm 30$ MeV fm^3 and $\beta \approx 100$ MeV fm^3, a result which is essentially consistent with proton elastic scattering.

I. INTRODUCTION

The elastic scattering of hadronic projectiles from nuclei has been a subject of experimental and theoretical studies for several decades. The main purpose of such investigations is to understand the mean field encountered by the projectile while traversing the nucleus. This field is usually described in terms of a complex optical model (OM) potential.

The OM potentials for the scattering of nucleons from a wide range of nuclei have been fairly well established from the lowest energies to about one GeV.[1] However, complications arise for complex projectiles such as ^{4}He and ^{6}Li due to the strong absorption of these projectiles by the nucleus. Low-energy elastic scattering of such projectiles ($E \lesssim 10$ MeV/nucleon) is thus sensitive only to the extreme surface region of the nucleus. Consequently, the data do not show much sensitivity to potentials in the interior region, and hence the OM potentials deduced from the data can be defined properly only for large radial distances.

Analyses of low-energy data have led to so-called discrete ambiguities in the potentials, first noticed for alpha particles by Igo.[2] It has also been found that potentials with distinctly different depths (varying in steps of ~ 50 MeV) provide equally acceptable fits to the ^{6}Li data.[3,4] For alpha particle scattering, measurements at sufficiently high bombarding energies ($E_\alpha \gtrsim 35$ MeV/nucleon) seem to have resolved these ambiguities in the OM potentials.[5] Measurements over wide angular ranges at the higher energies have provided differential cross sections beyond the diffraction region, in which oscillations are observed, into the refractive or so-called rainbow region, where the cross section exhibits a smooth exponential falloff with angle and no diffractive oscillations. The angle of transition between these two regions is normally referred to as the rainbow angle θ_R. In alpha particle scattering it has been found that measurements beyond θ_R are necessary and sufficient to select a unique potential from the discrete set of ambiguous choices.[6]

Extensive investigations of low-energy ^{6}Li elastic scattering have been carried out up to a bombarding energy of 50 MeV.[7] Data are also available for several targets at 73.7 MeV,[8] 88 MeV,[9] and 99 MeV.[3] Measurements were made on ^{28}Si at 135 MeV up to $\theta_{\rm c.m.} = 67°$.[4] At low bombarding energies, where θ_R is relatively large, it is very difficult to extend measurements into the rainbow region even for light nuclei and nearly impossible for heavy nuclei because of the rapid decrease of cross sections with angle. For example, for ^{28}Si at 135 MeV, θ_R is $\sim 67°$ and the cross section at that angle is

less than 1 μb/sr. Measurements on ^{28}Si at 154 MeV (Ref. 10) and on ^{12}C and ^{40}Ca at 156 MeV (Refs. 11 and 12) extend somewhat into the rainbow region. However, the extraction of unique potentials from these investigations may be questionable. Measurements on ^{90}Zr and ^{208}Pb at 156 MeV (Ref. 12) barely cover the diffraction regions.

In an effort to obtain unique OM potentials for ^{6}Li ions, we have measured differential cross sections for the elastic scattering of 210 MeV ^{6}Li ions on ^{12}C and ^{58}Ni targets over angular ranges extending well into the rainbow region ($\theta_R \sim 25°$ and 30° for ^{12}C and ^{58}Ni, respectively), thus allowing the derivation of unique OM potentials. Unique ^{6}Li potentials are of intrinsic interest because ^{6}Li is a projectile in the transition region between that characteristic of light-ion ($A \leq 4$) and heavy-ion (e.g., ^{12}C, ^{16}O) elastic scattering. Comparison of the results for ^{6}Li with those of the light ions and the heavy ions will provide a more systematic insight into the interactions between nuclei. Also, ^{6}Li is a feasible projectile for particle transfer reactions since, unlike heavier projectiles, it has no particle-stable strongly excited states. Thus, like heavy-ion reactions, it can transfer large amounts of angular momentum, and yet the spectra resemble light-ion reactions. However, to analyze the ^{6}Li-induced reactions one needs reliable OM parameters to generate the entrance channel distorted waves in reaction calculations.

Another concern relevant to the present data is the applicability of the various semimicroscopic potential-folding models for ^{6}Li elastic scattering. Both single-folding ^{6}Li potentials based on an $\alpha+$d cluster model[3,13] and double-folding potentials generated from realistic nucleon-nucleon interactions[14] have provided reasonable descriptions of lower energy data, although some renormalizations of the derived potentials have been necessary. Because of the higher energy and large angular range, the present data will provide a more stringent test of the existing folding models. This will be the subject of future investigations; the present work is concerned only with the phenomenological OM potential.

In Sec. II the experimental methods are described. The results of the measurements are presented in Sec. III. The OM analysis is discussed in Sec. IV. Finally, Sec. V contains the summary and conclusions of our investigation.

II. THE EXPERIMENT

The elastic scattering differential cross sections were measured using a 35 MeV/nucleon ^{6}Li beam at the National Superconducting Cyclotron Laboratory at Michigan State University. The uncertainty in the beam energy was estimated to be 1%, based on previous operating experience of the cyclotron and its extraction system. The targets were mounted at the center of a 40 cm diameter scattering chamber, and ranged in thicknesses from 0.5 to 20 mg/cm^2. Thin targets were used for the forward angle measurements where the yield for elastic scattering was large, and thick targets were used for measuring the low cross sections at large angles. The beam spot on target was usually 1 mm wide $\times$ 3 mm high. The beam current was varied between a fraction of a nA to over 200 nA (electrical), depending on the scattering angle, in order to keep the data acquisition dead time below 10%. The dead time was monitored by feeding pulses at a random rate to all detectors and processing the signals in the same manner as those from the real events in the detectors. The ratio of the number of processed pulses to those fed into the system was taken as the live time for each run. The real data were then corrected with these same live times.

Scattered particles were detected with a quadrupole-quadrupole-dipole-sextupole (QQDS) magnetic spectrometer[15] followed by a focal-plane detection system. The entrance slits to the spectrometer ranged from 35 to 660 μsr, depending on the angle of measurement. The corresponding angular resolution, $\Delta\theta$, was 0.35°–1.5°. The parameters of the spectrometer were adjusted at each scattering angle in order to maintain optimally focused elastically scattered ^{6}Li particles at the center of the focal plane. Since the energy bite of the spectrometer was about 20%, inelastic scattering up to $\sim$10 MeV excitation energy was also observed, and will be reported elsewhere.

The focal-plane detection system consisted of two resistive-wire proportional counters, two ion chambers, and a stopping plastic scintillator. All signals were processed by conventional electronics. A true event was defined by a coincidence between the front ion chamber and the plastic scintillator. The ion chambers, which served as energy loss ΔE counters, and the plastic scintillator, which stopped the ^{6}Li ions, were used for particle identification. They provided a clean separation between the ^{6}Li and ^{7}Li particles which arrived at the focal plane. A window on the two-dimensional display of these two detectors was used to gate the proportional counter spectra and thus the position on the focal plane (consequently the energy) of the scattered ^{6}Li particles was determined.

The angular position of the spectrometer could be read to an accuracy of 0.02°. The angular offset of the readout of the spectrometer was determined to be 0.10° by making elastic scattering measurements on both sides of the beam. The beam current was measured with two different Faraday cups. For angles $> 6°$, a counter-bored retractable Faraday cup which subtended an angle of 3° was used; for $\theta < 6°$ a Faraday cup fixed to the target chamber, which allowed measurements down to 2°, was used. Sufficient overlap data were taken with both cups to check the consistency between the two Faraday cup measurements.

The measurements were made by first increasing the scattering angle in large angular steps, and then taking intermediate points in the decreasing angle sequence. This procedure provides a check on long-term drifts in the experimental conditions (beam changes or target deterioration). However, no such drifts were observed. Enough data points were obtained in each angular distribution to adequately define the angular dependence of the cross sections. The criterion for each data point was to obtain statistical accuracy of at least 2% or a max-

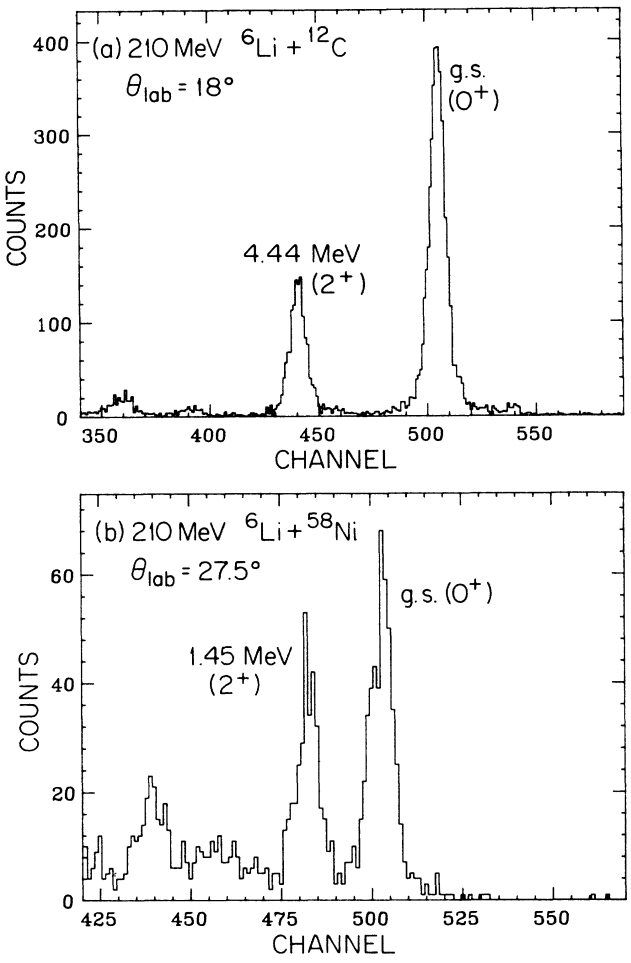

FIG. 1. Energy spectra for the scattering of 210 MeV ^{6}Li ions from ^{12}C at $\theta_{lab}=18°$ (a) and from ^{58}Ni at $\theta_{lab}=27.5°$ (b), showing the ground and first excited states.

imum data acquisition time of 30 min.

Several overlap points were taken with targets of different thicknesses. These data permitted correction of errors in target thickness measurements. The values for the thick targets were taken to be correct, and thicknesses of other targets were adjusted with the aid of the overlap data. Similar corrections were also made when spectrometer acceptance slits and beam current integrator scales were changed.

The overall energy resolution was typically 400–500 keV. This was sufficient to separate cleanly the ground state from the first excited state for the targets used. Spectra obtained for ^{12}C at $\theta_{lab}=18°$ and ^{58}Ni at $\theta_{lab}=27.5°$ are shown in Figs. 1(a) and (b).

Raw information for every event was recorded on magnetic tapes for off-line analysis.

III. RESULTS

Cross section measurements were made from 3° to 61° in the center of mass (c.m.) for ^{12}C; they ranged over eight orders of magnitude. The ^{58}Ni data covered nine orders of magnitude in the angular range 3°–48°. The results are shown in Figs. 2 and 3. The lowest cross section measured was 1 μb/sr.

The relative errors in the cross sections due to statistics are generally 1–2 %. Only for the largest angles do the errors exceed 10%. The uncertainty in the dead-time correction was kept below 1%. The uncertainty in the beam current charge collection was estimated to be ~1%. The error introduced by the variation in the beam position on the target (due to nonuniformity of the target thickness) ranged from ~3% for the thin targets to ~0.5% for the thick targets. The uncertainty in effective scattering angle due to variation in beam direction during measurements was estimated to be about 0.04°. This introduced an additional relative error of up to 8% depending on the slope of the cross section. The relative errors from all sources were added in quadrature for each data point. These values ranged from ~3% to ~12%, and are displayed in Figs. 2 and 3 when the errors are larger than the data points. Differences in repeated measurements also indicated that the minimum error is ~3%. The absolute (systematic) error for each angular distribution due to uncertainties in target thickness, spectrometer solid angle, and charge integration was estimated to be ~10%.

Figure 2 shows that for ^{12}C, diffractive oscillations are observed at small angles but a transition to refractive scattering occurs at a rainbow angle $\theta_R \sim 25°$. For ^{58}Ni one observes diffraction scattering up to ~30°, and rainbow scattering at larger angles.

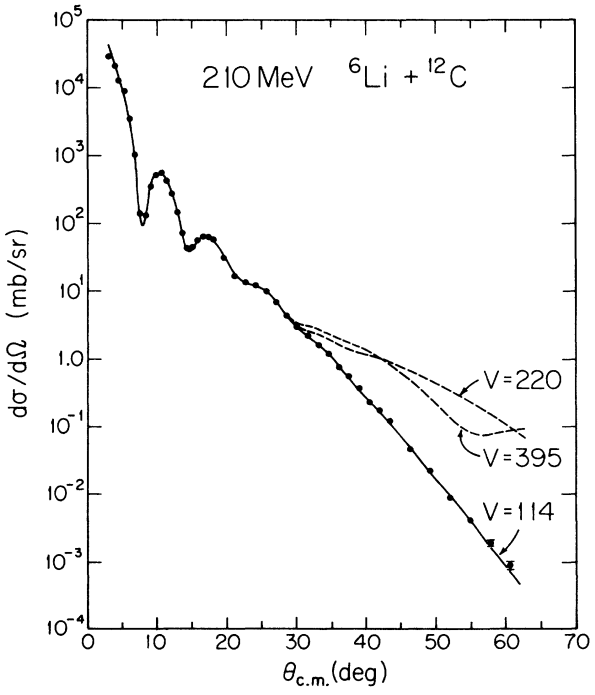

FIG. 2. Differential cross section angular distribution for the elastic scattering of 210 MeV ^{6}Li ions from ^{12}C. The solid curve is the optical model fit that provides the unique potential listed in Table I. The dashed lines represent calculations with the ambiguous potentials given in Table II.

IV. OPTICAL MODEL ANALYSES

The OM analyses were initially carried out with the code SNOOPY8.[16] This program provided good fits for the ^{12}C data but was unable to perform the calculations for ^{58}Ni because the maximum number of partial waves (100) allowed for in the code was insufficient for these data.

Calculations for the ^{58}Ni target were, therefore, carried out with the code ECIS79,[17] which has no partial wave limitation for the present data. As a cross check for computational accuracy, the ^{12}C data were also reanalyzed with ECIS79. The results obtained from both codes were found to be essentially identical.

The optical potential used to fit the data was of the conventional form, consisting of a complex central term with Woods-Saxon form factors (volume and surface absorption) and a Coulomb term. The form of the potential was

$$U(r)=-Vf_0(r)-i[W_v-4a_wW_s(d/dr)]f_w(r)+U_c(r) ,$$

where

$$f_x(r)=\{1+\exp[(r-r_xA^{1/3})/a_x]\}^{-1} ,$$

No spin-orbit potential term was included since the relatively weak spin-orbit interaction for ^{6}Li has little influence on the differential cross section.

The Coulomb potential was taken to be that of a uniformly charged sphere with a charge equal to Ze of the target nucleus and a radius equal to $R=r_cA^{1/3}$, where $r_c=1.2$ fm. Thus the Coulomb potential had the form

$$V(r)=\frac{Ze}{8\pi\varepsilon_0R}\left[3-\frac{r^2}{R^2}\right], \quad \text{for } r\le R ,$$

and

$$V(r)=\frac{Ze}{4\pi\varepsilon_0r}, \quad \text{for } r\ge R .$$

Initial searches were carried out with only a volume absorption potential (W_v). The starting parameters were taken from the various sets of the 99 MeV analyses.[3] Searches were made on various combination of the six parameters to minimize χ^2, defined by

$$\chi^2=\sum_{i=1}^{N}\frac{(\sigma_i^{\text{cal}}-\sigma_i^{\text{exp}})^2}{\Delta\sigma_i^2} ,$$

where σ_i^{cal} is the calculated cross section and σ_i^{exp} and $\Delta\sigma_i$ represent the experimental cross section and its uncertainty, respectively. N is the number of data points. When a minimum χ^2 value was reached, a surface absorption component (W_s) was introduced and searches were then made on all seven parameters. It was found that while the parameter values readjusted, practically no improvement in the quality of the fit in terms of the χ^2 criterion or visual observation was obtained. Since the introduction of an additional parameter produced essentially no improvement, the surface term was set to zero. The final parameters thus obtained are listed in Table I. Fits to the data are shown as solid lines in Fig. 2 and 3.

By gridding on the strength of the real potential and varying the other five parameters, searches were made to obtain other potential families. No other families were found for V_0 ranging from 40 to 500 MeV. Thus it was concluded that the derived potentials are unique for the data.

An attempt was made to determine the maximum angular range of the data for which ambiguous potentials still exist. This was done by successive elimination of large angle data, until acceptable fits could be obtained for other potential sets. It was found that if the data for the ^{12}C angular distribution are limited to 29°, several additional potentials provide equally good fits. These analyses were carried out by gridding on the strength (V) of the real potential from 40 to 500 MeV in steps of 5 MeV, and searching on all the other five parameters. The results are displayed in Fig. 4. It is observed that χ^2/N (dashed line) remains essentially constant over the entire range, with three shallow minima. These minima correspond to the best fit for the three distinct families of volume integrals ($\sim$300, 400, and 500 MeV fm^3), shown by the solid line. Also shown in Fig. 4 are the χ^2/N values for the full data set (dot-dashed line). They illustrate that the full data set selects the unique potential for ^{6}Li+^{12}C at 210 MeV.

The ambiguous sets of parameters for the other two minima in Fig. 4 are listed in Table II. Differential cross section calculations were made for the entire angular distribution using new parameters. These are shown as dashed lines in Fig. 2. Similarly for the ^{58}Ni data, the angular distribution up to 27° yields ambiguous potentials. Three such parameter sets are listed in Table II and the corresponding calculations are shown as dashed lines in Fig. 3.

It is observed that cross sections calculated from the ambiguous potentials deviate substantially from the data for angles beyond the cutoff angle (29° or 27°). Thus the large-angle data are essential for eliminating the ambiguities in the potentials. These results emphasize the importance of making large angle measurements at sufficiently high bombarding energies in order to deter-

TABLE I. Best fit potential parameters for elastic scattering of 210 MeV ^{6}Li ions from ^{12}C and ^{58}Ni. The convention $R_x=r_xA^{1/3}$ is used.

Target	V (MeV)	r_0 (fm)	a_0 (fm)	W_v (MeV)	r_W (fm)	a_w (fm)	$J_R/6A$ (MeV fm^3)	$J_W/6A$ (MeV fm^3)	σ_R (mb)	χ^2/N
^{12}C	113.5	1.305	0.793	34.2	1.682	0.784	298	160	1090	3.9
^{58}Ni	174.5	1.136	0.907	32.0	1.607	0.806	253	108	2084	10.2

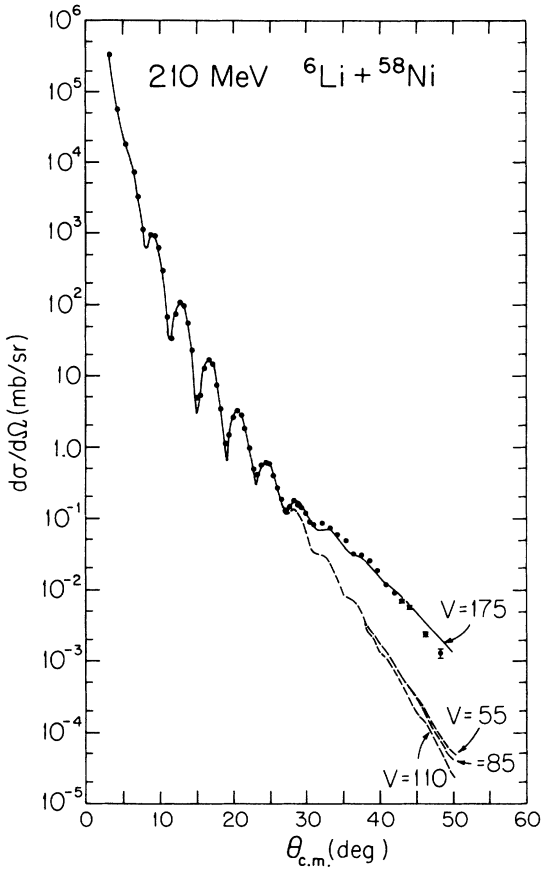

FIG. 3. Same as Fig. 2, but for a ^{58}Ni target.

mine unique OM parameters for the elastic scattering of ^{6}Li particles.

V. SUMMARY AND CONCLUSIONS

Measurements of differential cross sections for the elastic scattering of 210 MeV ^{6}Li ions have been made for ^{12}C ($\theta_{c.m.}=3°-61°$) and ^{58}Ni ($\theta_{c.m.}=3°-48°$). The angular ranges are sufficiently extensive for the determination of unique OM potentials while calculations with truncated data sets (over a limited angular range) result in ambiguous potential sets. Clearly, measurements at angles well into the rainbow region are required in order to select the correct potentials from the various

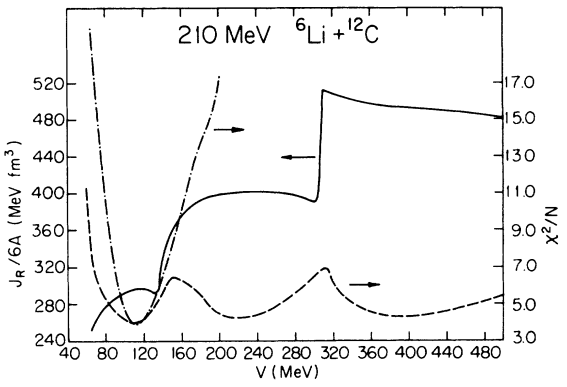

FIG. 4. Results of optical model analyses of the truncated data set for ^{12}C. The solid line is the volume integral per nucleon pair ($J_R/6A$) as a function of the strength (V) of the real potential (scale on left-hand side). Three distinct families are observed. The dashed line represents the corresponding χ^2 values (right-hand scale). The dot-dashed line shows the χ^2 values for the full data set, which selects the correct potential family.

families. Thus, unique potential parameters for the ^{6}Li-^{12}C and ^{6}Li-^{58}Ni interactions at 210 MeV have been obtained for the first time.

It is now possible to extrapolate these values to lower energies, thus resolving the ambiguity problems previously associated with the low energy data. Such an attempt is shown in Fig. 5. The volume integrals per nucleon pair ($J_R/6A$) of the real potential from the present and published analyses[3,12,18] are shown as dots for ^{12}C [Fig. 5(a)] and ^{58}Ni [Fig. 5(b)] as a function of the bombarding energy. For ^{12}C, the present results along with results from analyses at 156 MeV (Ref. 12) and 99 MeV (Ref. 3) provide the guide for extrapolation to lower energies. The volume integrals clearly follow a logarithmic energy dependence of the form

$$J_R/6A = J_R^0/6A - \beta \ln E_{\rm lab}$$

with $J_R^0/6A = 830\pm30$ MeV fm^3 and $\beta \approx 100\pm5$ MeV fm^3. This is shown by the solid line in Fig. 5(a). The extrapolation of the ^{58}Ni potential used a value obtained from a recent reanalysis of the 99 MeV data.[19] The volume integrals again follow a logarithmic energy dependence with $J_R^0/6A = 800\pm30$ MeV fm^3 and

TABLE II. Additional parameter sets describing truncated angular distribution data of 210 MeV ^{6}Li ions. The convention $R_x = r_x A^{1/3}$ is used.

Target	V (MeV)	r_0 (fm)	a_0 (fm)	W_v (MeV)	r_W (fm)	a_w (fm)	$J_R/6A$ (MeV fm^3)	$J_W/6A$ (MeV fm^3)	σ_R (mb)	χ^2/N
^{12}C	220.0	1.118	0.760	42.0	1.541	0.835	401	166	1105	4.2
^{12}C	395.0	0.918	0.762	42.3	1.540	0.831	493	167	1102	4.3
^{58}Ni	55.0	1.486	0.782	59.6	1.407	0.862	149	144	2157	3.6
^{58}Ni	85.0	1.354	0.837	62.9	1.409	0.847	184	152	2069	4.3
^{58}Ni	110.0	1.273	0.860	57.1	1.447	0.825	206	146	2057	6.3

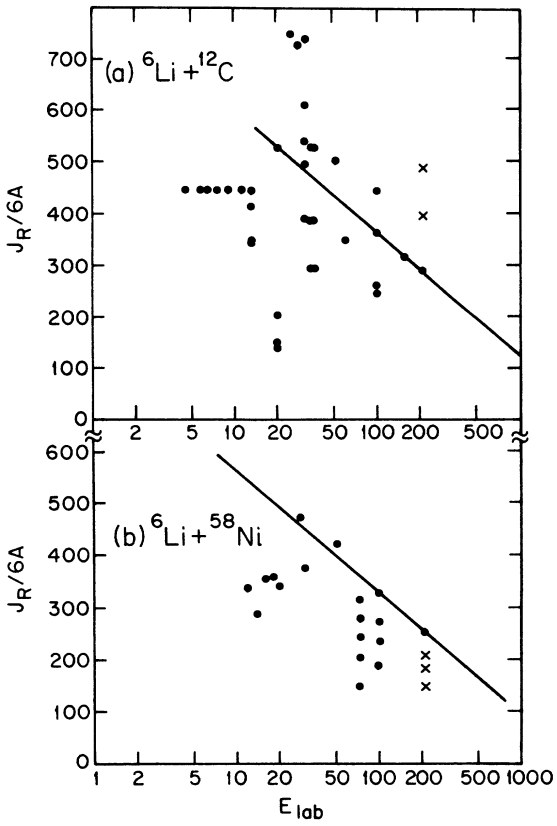

FIG. 5. Energy dependence of the volume integrals for the elastic scattering of ^{6}Li from ^{12}C (a) and ^{58}Ni (b). The solid lines are extrapolations of the present unique potentials at 210 MeV to lower energies. The $\times$'s represent the ambiguous potentials obtained with the truncated data sets. They seem to correspond to other families found at lower energies.

$\beta = 100 \pm 5$ MeV fm^3, shown as a solid line in Fig. 5(b). The volume integrals of the ambiguous potentials obtained from the truncated data sets are shown as crosses in Fig. 5. If one assumes the same energy dependence for these potentials with a different $J_R^0/6A$, it is observed that they correspond to other families found at lower energies.

The $J_R^0/6A$ obtained in both cases are in excellent agreement with the proton elastic scattering results of Nadasen *et al.*[1] (815 ± 15 MeV fm^3), but, as expected, the energy dependence is weaker. According to the above energy dependences, the ^{6}Li-nucleus real potential is expected to become zero at an energy of 3500 ± 500 MeV. In terms of energy per projectile nucleon, the ^{6}Li value ($\simeq 600 \pm 100$ MeV/nucleon) agrees well with the 600 MeV value found for protons in analyses using Woods-Saxon potential form factors.[20] The imaginary volume integrals for both ^{12}C and ^{58}Ni are not sensitive to the potential ambiguities. They remain essentially constant with $J_W/6A \simeq 140 \pm 30$ MeV fm^3 for all values of V.

The total reaction cross sections, σ_R, have been calculated from the various sets of optical potentials. These are indicated in Tables I and II. The values of ~ 1100 mb and ~ 2100 mb for ^{12}C and ^{58}Ni, respectively, are about twice as large as those for nucleon-nucleus scattering[1,21] at comparable energies per nucleon, in agreement with lower energy ^{6}Li elastic scattering.[7]

Finally, since unique phenomenological OM potentials have been obtained for the ^{6}Li + nucleus interaction at 210 MeV and their energy dependence has been established, it is now possible to evaluate the various prescriptions for the potential-folding models. This will be the subject of future investigations.

ACKNOWLEDGMENTS

We thank the operations group at National Superconducting Cyclotron Laboratory (NSCL) for the high quality ^{6}Li beams provided for this experiment. This work was supported in part by the National Science Foundation under Grants PHY 8304886 and PHY 8308072 (University of Michigan), PHY 8412177 (Indiana University Cyclotron Facility), PHY 8611210 (NSCL), and PHY 8521042 (Oberlin College).

*Present address: Department of Physics, University of Groningen, 9718CM Groningen, The Netherlands.

[1] A. Nadasen *et al.*, Phys. Rev. C **23**, 1023 (1981); W. T. H. van Oers *et al.*, *ibid.* **10**, 307 (1974); F. D. Becchetti and G. W. Greenlees, Phys. Rev. **182**, 1190 (1969).

[2] G. Igo, Phys. Rev. **115**, 1665 (1959); Phys. Rev. Lett. **1**, 72 (1958).

[3] P. Schwandt *et al.*, Phys. Rev. C **24**, 1522 (1981).

[4] R. M. DeVries, D. A. Goldberg, J. W. Watson, M. S. Zisman, and J. G. Cramer, Phys. Rev. Lett. **39**, 450 (1977).

[5] S. M. Smith *et al.*, Nucl. Phys. **A207**, 273 (1973); D. A. Goldberg, S. M. Smith, H. G. Pugh, P. G. Roos, and N. S. Wall, Phys. Rev. C **7**, 1938 (1973).

[6] D. A. Goldberg and S. M. Smith, Phys. Rev. Lett. **29**, 500 (1975); D. A. Goldberg, S. M. Smith, and G. F. Burdzik, Phys. Rev. C **10**, 1397 (1974).

[7] L. T. Chua, F. D. Becchetti, J. Jänecke, and F. L. Milder, Nucl. Phys. **A273**, 243 (1976), and references therein.

[8] R. Huffman, A. Galonsky, R. Markham, and C. Williamson, Phys. Rev. C **22**, 1522 (1980).

[9] C. B. Fulmer *et al.*, Nucl. Phys. **A356**, 235 (1981).

[10] P. Schwandt, S. Kailas, W. W. Jacobs, M. D. Kaitchuck, W. Ploughe, and P. P. Singh, Phys. Rev. C **21**, 1656 (1980).

[11] Z. Majka, H. J. Gils, and H. Rebel, Z. Phys. A **288**, 139 (1978).

[12] J. Cook, H. J. Gils, H. Rebel, Z. Majka, and H. Klewe-Nebenius, Nucl. Phys. **A388**, 173 (1982).

[13] P. Schwandt *et al.*, Phys. Rev. C **21**, 1656 (1980); J. Jänecke, F. D. Becchetti, and D. Overway, Nucl. Phys. **A343**, 161 (1980).

[14] D. P. Stanley, F. Petrovich, and P. Schwandt, Phys. Rev. C **22**, 1357 (1980); G. R. Satchler and W. G. Love, Phys. Rep. **55**, 183 (1979).

[15] B. M. Sherrill, Ph.D. thesis, Michigan State University, 1985.

[16]P. Schwandt, Indiana University Cyclotron Facility Report 82-3, 1982.
[17]J. Raynal, computer code ECIS79 (unpublished).
[18]J. Cook, At. Data Nucl. Tables **26**, 19 (1981); C. M. Perey and F. G. Perey, *ibid.* **17**, 92 (1976).
[19]P. Schwandt (unpublished).
[20]P. Schwandt, in *The Interaction Between Medium Energy Nucleons in Nuclei-1982 (Indiana Cyclotron Facility, Bloomington, Indiana),* Proceedings of the Workshop on the Interactions Between Medium Energy Nucleons in Nuclei, AIP Conf. Proc. No. 97, edited by H. O. Meyer (AIP, New York, 1982), p. 89.
[21]J. J. H. Menet, E. E. Gross, J. J. Malanify, and A. Zucker, Phys. Rev. C **4**, 1114 (1971).